Molecular Pharmacology Fast Forward. Published on September 20, 2006 as doi:10.1124/mol.106.029215
This article has not been copyedited and formatted. The final version may differ from this version.

MOL #29215

Endogenous Hepatic Expression of the Hepatitis B Virus X-associated Protein 2 is Adequate for Maximal Association with Aryl Hydrocarbon Receptor-HSP90 Complexes

Authors: Brett D. Hollingshead, Rushang D. Patel, Gary H. Perdew

Graduate Program in Biochemistry, Microbiology, and Molecular Biology (BDH) and The Department of Veterinary and Biomedical Sciences and The Center for Molecular Toxicology and Carcinogenesis, The Pennsylvania State University, University Park, PA, U.S.A. (BDH, RDP, and GHP)

Molecular Pharmacology Fast Forward. Published on September 20, 2006 as DOI: 10.1124/mol.106.029215
This article has not been copyedited and formatted. The final version may differ from this version.

Running Title: *In vivo* modulation of the AHR by XAP2

Corresponding Author:
Gary H. Perdew
The Center for Molecular Toxicology and Carcinogenesis
309 Life Sciences Building
The Pennsylvania State University
University Park, PA 16802
U.S.A
Telephone: (814) 865-0400
Fax: (814) 863-1696
e-mail: ghp2@psu.edu

Number of:
Text pages: 25
Tables: 2
Figures: 7
References: 40
Words in abstract: 247
Words in introduction: 744
Words in discussion: 1369

Abbreviations:

AHR, aryl hydrocarbon receptor; XAP2, hepatitis B virus X-associated protein 2; HSP90, 90 kDa heat shock protein; TCDD, 2,3,7,8-tetrachlorodibenzo-p-dioxin; bHLH PAS, basic helix-loop-helix Per/ARNT/Sim; MENG, 25 mM MOPS, 2 mM EDTA, 0.02% NaN_3, and 10% glycerol (pH=7.5); PVDF, polyvinylidene difluoride; QRT-PCR, quantitative real-time PCR; TSDS-PAGE, Tricine SDS polyacrylamide gel electrophoresis; NP-40, Nonidet P-40; CYP, cytochrome P450; NQO1, NAD(P)H dehydrogenase, quinone 1; UGT1A2, UDP-glucuronosyltransferase 1A2; CAR, constitutive androstane receptor; NRF2, nuclear factor erythroid 2-related factor 2; FABPL, liver fatty acid binding protein; ACOX1, acyl-Coenzyme A oxidase 1

Molecular Pharmacology Fast Forward. Published on September 20, 2006 as DOI: 10.1124/mol.106.029215
This article has not been copyedited and formatted. The final version may differ from this version.

Abstract

The aryl hydrocarbon receptor (AHR) is a ligand activated transcription factor that acts as an environmental sensor by binding to a wide variety of xenobiotics. AHR activation serves to combat xenotoxic stress by inducing metabolic enzyme expression in the liver. The hepatitis B virus X-associated protein (XAP2) is a component of the cytosolic AHR complex and modulates AHR transcriptional properties *in vitro* and in cell culture and yeast systems. Expression of XAP2 is low in liver compared to other non-hepatic tissues and the AHR exhibits high ligand-induced transcriptional activity. Since XAP2 has been demonstrated to repress AHR activity, we hypothesized that XAP2 may be limiting in liver and that increasing XAP2 levels would attenuate AHR transcriptional activity. To this end transgenic mice were generated that exhibit hepatocyte-specific elevation in XAP2 expression. Transgenic XAP2 expression was restricted to liver, and its ability to complex with the AHR was verified. Gene expression experiments were performed by inducing AHR transcriptional activity with β-napthoflavone via intraperitoneal injection, and mRNA quantification was done by real-time PCR. Wild-type and transgenic animals showed little difference in constitutive or ligand-induced CYP1A1, CYP1A2, UGT1A2, NQO1, CAR, or NRF2 mRNA expression. Sucrose density fractionation and AHR immunoprecipitation experiments found little or no stoichiometric increase in bound XAP2 to the AHR between genotypes. Gene array studies were performed to identify novel XAP2-regulated targets. Taken together, this work shows that despite the relatively low level of XAP2 in liver, it is not a limiting component in AHR regulation.

Molecular Pharmacology Fast Forward. Published on September 20, 2006 as DOI: 10.1124/mol.106.029215
This article has not been copyedited and formatted. The final version may differ from this version.

The aryl hydrocarbon receptor (AHR) is a soluble, ligand-activated transcription factor that mediates the metabolic clearance, and at times the procarcinogenic biotransformation, of xenobiotics and endogenous compounds through the transcriptional induction of phase I and II metabolic enzymes such as the cytochrome P450's 1A1, 1A2, and 1B1, as well as UDP-glucuronosyltransferase, NAD(P)H:oxidoreductase, and glutathione S-transferase Ya subunit (as reviewed in (Nebert et al., 2000)). In rodent models numerous toxic effects have been observed to be mediated through AHR activation, including cancer, liver toxicity, thymic atrophy, and teratogenesis. These effects are elicited through exposure to the high affinity and metabolically resistant AHR ligand, 2,3,7,8-tetrachlorodibenzo-*p*-dioxin (TCDD) and, to some extent, polycyclic aromatic hydrocarbons such as benzo[*a*]pyrene. The generation of AHR null mouse strains (Fernandez-Salguero et al., 1995; Schmidt et al., 1996) has established that most of the deleterious effects observed through TCDD exposure are mediated through the AHR, as these animals are refractory to TCDD-induced toxicity.

The AHR is a member of the basic helix-loop-helix PER/ARNT/SIM (bHLH-PAS) family of transcription factors. Members of the bHLH-PAS family tend to be involved in maintaining homeostasis, such as regulating circadian rhythms (Panda et al., 2002) and alleviating hypoxia (Kewley et al., 2004). Although the physiological role for the AHR has yet to be fully understood, studies involving AHR null mice have revealed that the receptor is an important player in regulating pathways involved in maturation of fetal vasculature in the developing liver (Lahvis et al., 2000; Walisser et al., 2004). Additionally, reduced fertility is observed in AHR null females, which has recently been suggested to be attributed to the deregulation of estradiol production through altered

CYP19 gene expression in ovarian granulosa cells (Baba et al., 2005). AHR-deficient mice also display a propensity for the development of liver fibrosis, due to the impaired ability to maintain retinoid homeostasis (Andreola et al., 2004). Age-dependent formation of lesions in multiple organs of AHR null mice have also been reported, implying that the AHR is necessary in maintaining homeostasis throughout life (Fernandez-Salguero et al., 1997).

The AHR, in its inactive form, exists in the cytoplasm as a complex consisting of a dimer of HSP90 (Chen and Perdew, 1994), and potentially at least one molecule of the co-chaperones XAP2 (Carver and Bradfield, 1997; Ma and Whitlock, 1997; Meyer et al., 1998) and p23 (Kazlauskas et al., 1999; Nair et al., 1996). HSP90 is an essential component of the unliganded AHR complex, and its presence is necessary to maintain optimal ligand-binding capacity (Carver et al., 1994; Pongratz et al., 1992). The capability of XAP2, also known as AIP (Ma and Whitlock, 1997) or ARA9 (Carver and Bradfield, 1997), to modulate AHR function has been studied extensively in cell culture systems. Through the use of yeast and mammalian cell culture systems XAP2 has been demonstrated to regulate AHR transcriptional activity, cellular localization, and overall stability (Petrulis and Perdew, 2002). However, there are discrepancies between reports as to how XAP2 serves to modulate AHR function. For example, some studies report XAP2-mediated enhancement of AHR transcriptional output (Carver et al., 1998; LaPres et al., 2000; Ma and Whitlock, 1997), while others suggest that XAP2 exerts repressive properties on AHR transcriptional activity (Hollingshead et al., 2004; Pollenz and Dougherty, 2005). Additionally, it has been reported that XAP2 stabilizes the AHR from proteosome-mediated degradation (Kazlauskas et al., 2000; Lees et al., 2003), while

others maintain that XAP2 only exerts a modest influence in sustaining receptor levels (Hollingshead et al., 2004; Pollenz and Dougherty, 2005).

Previous studies have utilized mammalian cell culture, yeast, or *in vitro* systems to examine XAP2-mediated regulation of the AHR, often resulting in contradictory results. Because of this it is necessary to study XAP2 function in the context of regulating the AHR in an *in vivo* setting. There is considerable variation in XAP2 expression within different tissues, and it is particularly low in the liver (Meyer et al., 1998). The AHR's ability to induce metabolic gene expression in the liver has been firmly established. Considering that XAP2 expression is relatively low in the liver combined with the understanding that the AHR is transcriptionally active in response to ligand, we wanted to see if increasing the expression of XAP2 in the liver would serve to modify AHR behavior. This would allow us to elucidate whether differing amounts of XAP2 in tissues could be a mechanism of finely controlling AHR activity. To that end, transgenic mouse lines that display increased XAP2 expression in the liver under the transcriptional control of a hepatocyte specific promoter were generated. This study describing the effects of increased XAP2 expression on AHR function are the first *in vivo* experiments of this nature to be performed to date.

Molecular Pharmacology Fast Forward. Published on September 20, 2006 as DOI: 10.1124/mol.106.029215
This article has not been copyedited and formatted. The final version may differ from this version.

Materials and methods

Construction of mXAP2-FLAG transgenic mice

PCR primers were designed (5′-CATGGATATCGCCGCCATGGCGGATCTCATCG-3′ and 5′-CATGGATATCTC ACTTGTCATCGTCGTCCTTGTAGTCGTGGGAAAAGATGCC-3′) to amplify the mouse XAP2 cDNA to incorporate the FLAG amino acid sequence on the C-terminus. The PCR product contained EcoRV sites on the 5′ and 3′ ends of the mXAP2-FLAG PCR product. The amplified fragment was digested with EcoRV and blunt-end ligated into the StuI site of the TTR1ExV3 vector (a gift from Dr. Terry Van Dyke, (Wu et al., 1996)) creating the plasmid TTR1ExV3/XAP2-FLAG. The TTR1ExV3/XAP2-FLAG vector was sequenced to validate that the XAP2-FLAG sequence and orientation of insertion in the plasmid was correct. The TTR vector is under the transcriptional control of the liver specific transthyretin promoter allowing for controlled expression of the transgene in hepatocytes.

The TTR1ExV3/XAP2-FLAG construct was digested with HINDIII and the 5.4 kb transgene fragment was purified and injected into C57BL/6J fertilized eggs at the Penn State transgenic facility. Founder mice and offspring were screened using PCR and QRT-PCR assays described below. C57BL/6J mice used to derive transgenic lines, and subsequently propagate animal colonies were from Jackson Labs (Bar Harbor, Maine). $AHR^{-/-}$ mice were obtained from Dr. Christopher Bradfield (University of Wisconsin). Mice were maintained in a temperature-controlled facility on 12 h light/dark cycle and were given ad libitum access to food and water.

Molecular Pharmacology Fast Forward. Published on September 20, 2006 as DOI: 10.1124/mol.106.029215
This article has not been copyedited and formatted. The final version may differ from this version.

Screening of transgenic mice

Mice were screened using tail DNA isolated with the Wizard® SV genomic DNA purification kit (Promega). Presence of the XAP2-FLAG transgene in mice was determined by PCR using primers (see Fig. 1B) specific for the transgene (primer set 1: 5′- CCCAGGGTGCTGGAGAGGATCGCCGCC-3′ and 5′-GCGGAGGCTCTTGGCCACTAGAGG-3′; primer set 2: 5′-GCCAGTGCAAGCTGGTGGCTCAGGAG-3′ and 5′-CGTCGTCCTTGTAGTCGTGGG-3′).

In order to genotype transgenic animals, and estimate transgene copy number QRT-PCR was used (primer set: 5′-ACGCTGCACAGTGACAATGAA-3′ and 5′-CTCCCACACAGGCAACTTGA-3′). This primer set amplifies a 104bp DNA fragment located within exon 2 of the XAP2 gene allowing for the amplification of the endogenous XAP2 and transgenic XAP2-FLAG genes simultaneously. QRT-PCR reactions were run using the DyNAmo™ SYBR® Green qPCR kit (Finnzymes) on a MJ Research Opticon DNA engine (Bio-Rad). Genotyping was performed by using tail DNA from a hemizygous transgenic animal to generate a standard curve (50-0.05 ng). Additionally, reactions using 5 ng of template DNA were used for unknown transgenic genomic samples, and the relative amount of XAP2 was determined within each founder line. Hemizygous (XAP2-FLAG$^{+/-}$) and homozygous (XAP2-FLAG$^{+/+}$) mice were identified by an equal or 2-fold increase in XAP2 signal, respectively, as compared to the hemizygous standard. Transgene copy number was estimated by examining the fold increase in XAP2 signal in hemizygous versus wild-type mice. Transgene copy number

Molecular Pharmacology Fast Forward. Published on September 20, 2006 as DOI: 10.1124/mol.106.029215
This article has not been copyedited and formatted. The final version may differ from this version.

was found to be the same (5-6 copies) for each mouse line (Tg04 and Tg18) used in this study.

Gene expression following exposure to an AHR ligand

The generation of CYP1A1 mRNA dose-response curves following the exposure to the AHR ligand β-naphthoflavone (β-NF) were performed in a similar manner as was used previously for monitoring aryl hydrocarbon hydroxylase activity (Niwa et al., 1975). Male wild-type (non-transgenic C57BL/6J), $Tg04^{+/+}$, and $Tg18^{+/+}$ animals between six and ten weeks of age were intraperitoneally injected with corn oil alone or β-NF (Sigma) dissolved in corn oil at concentrations ranging from 1×10^{-3} to 2.5×10^{2} mg/kg. 6 h after β-NF treatment mice were euthanized by asphyxiation due to CO_2 exposure. Livers were excised, washed in cold PBS, weighed, and ~50-100 mg pieces were taken from the left lobe and snap frozen in liquid nitrogen. Female ten week old $AHR^{-/-}$ mice were administered 50 mg/kg β-NF for 5 h. Samples were stored at -80° C until used for RNA isolation. Frozen tissues were homogenized with an Ultra Turrax T25 basic disperser (IKA® Works, Inc.) in TRI Reagent (Sigma), and RNA was isolated as specified by the manufacturer. The ABI high-capacity cDNA archive kit (Applied Biosystems) was used to prepare cDNA from isolated tissue RNA.

Measurements of mRNA expression for all samples were performed by QRT-PCR using the DyNAmo™ SYBR® Green qPCR kit on an MJ Research Opticon DNA engine. A common standard cDNA sample, generated from a 10 mg/kg β-NF treated wild-type mouse, was used for all real time PCR reactions so that data points collected between runs could be directly compared. Individual expression values for each gene

Molecular Pharmacology Fast Forward. Published on September 20, 2006 as DOI: 10.1124/mol.106.029215
This article has not been copyedited and formatted. The final version may differ from this version.

were normalized to GAPDH levels within each sample. Primer sequences used for the quantification of CYP1A1 mRNA were 5′-CTCTTCCCTGGATGCCTTCAA-3′ and 5′-GGATGTGGCCCTTCTCAAATG-3′

Additionally, the expression of CYP1A2 (5′-ACATTCCCAAGGAGCGCTGTATCT-3′ and 5′-GTCGATGGCCGAGTTGTTATTGGT-3′), NQO1 (5′-AGATGGCATCCAGTCCTCCAT-3′ and 5′-TTAGTCCCTCGGCCATTGTT-3′), UGT1A2 (5′-AAGGCTTTCTGACCACATGGA-3′ and 5′-GGCAAATGTACTTCAGGACCAGAT-3′), GAPDH (5′-CATGGCCTTCCGTGTTCCTA-3′ and 5′-GCGGCACGTCAGATCCA-3′), CAR (5′-GGAGCGGCTGTGGAAATATTGCAT-3′ and 5′-TCCATCTTGTAGCAAAGAGGCCCA-3′), and NRF2 (5′-AGCACTCCGTGGAGTCTTCCATTT-3′ and 5′-TGTGCTTTAGGGCCGTTCTGTTTG-3′) were assessed at β-NF concentrations of 0, 20, and 250 mg/kg. Data was plotted and statistical analysis (*F* test for CYP1A1 dose-response, two-way ANOVA with Bonferroni post-test for other gene expression) was performed using GraphPad Prism 4.00 (GraphPad Software).

Gene expression following exposure to a PPARα ligand

Eight to ten week old wild-type or Tg04$^{+/+}$ males were left untreated, or administered the PPARα specific ligand WY-14,643 (50 mg/kg) or corn oil vehicle via gavage. 7 h after treatment mice were euthanized by asphyxiation due to CO_2 exposure. Livers were excised, washed in cold PBS, and ~50-100 mg pieces were taken from the

Molecular Pharmacology Fast Forward. Published on September 20, 2006 as DOI: 10.1124/mol.106.029215
This article has not been copyedited and formatted. The final version may differ from this version.

left lobe and snap frozen in liquid nitrogen. RNA was isolated and QRT-PCR performed as described above. QRT-PCR primer sets used for the PPARα regulated genes ACOX1 and FABPL were as follows: ACOX1 (5′-GTCGACCTTGTTCGCGCA-3′ and 5′-GGTTCCTCAGCACGGCTTG-3′), FABPL (5′-AGCCAGGAGAACTTTGAGCCA-3′ and 5′-CATGCACGATTTCTGACACCC-3′).

Liver cytosol and whole cell extract preparation

To prepare cytosol animals were euthanized by asphyxiation with CO_2, after which livers were removed and washed with cold PBS. Tissue pieces were disrupted (100 mg per 1 ml buffer) using a glass-teflon homogenizer in a buffer composed of MENG supplemented with 20 mM Na_2MoO_4 and 1X protease inhibitor cocktail (Sigma). Cytosol was then obtained by centrifuging the crude homogenate at 100,000 x g for 1 h.

Whole cell extracts were prepared by homogenizing frozen tissues in RIPA buffer using a glass-teflon homogenizer. Homogenates were centrifuged at 21,000 x g for 45 min and supernatant was collected. Protein content was determined in whole cell extracts with a detergent compatible protein assay kit (Bio-Rad).

AHR and FLAG immunoprecipitations

To immunoprecipitate the AHR 75 μg (~10-20 μl) of cytosol was mixed in 500 μl of binding buffer (MENG, 20 mM Na_2MoO_4, 0.1% NP-40, 1.0 mg/ml BSA) followed by the addition of either 4 μg anti-AHR polyclonal IgG (Biomol) or non-specific IgG (Sigma). Cytosol was allowed to mix with the antibody for 2 h at 4° C, after which 30 μl of anti-rabbit IgG agarose (Sigma) was added to each sample. Immunoprecipitation

reactions were then mixed at 4° C for 1 h followed by three washes with a buffer consisting of MENG, 20 mM Na_2MoO_4, 0.1% NP-40, and 50mM NaCl, and finally one wash with MENG plus 20 mM Na_2MoO_4.

Immunoprecipitations of XAP2-FLAG from transgenic cytosols were performed by adding 50 μg (~10-20 μl) of cytosol to 750 μl of binding buffer. That mixture was then allowed to mix with 30 μl of anti-FLAG M2-agarose affinity gel (Sigma) at 4° C for 2 h followed by three washes with the same buffer used in the AHR immunoprecipitation washes. Samples were resolved by 8% TSDS-PAGE, and transferred to PVDF membrane (Millipore). Proteins were visualized by immunoblot using the following antibodies: AHR (RPT-1 (Affinity BioReagents)), XAP2 (ARA-9 monoclonal (Novus Biologicals)), and FLAG (anti-FLAG (Affinity BioReagents)). Biotin conjugated secondary antibodies (Jackson Immunoresearch) in conjunction with ^{125}I-streptavidin (Amersham Biosciences, Piscataway, NJ) were used and autoradiograms were visualized using Biomax MS film (Eastman Kodak).

For silver stain analysis FLAG immunoprecipitations were carried out essentially as described above except a total of 2 mg of cytosolic protein was applied to the anti-FLAG resin and adsorbed complexes were eluted off of the resin using FLAG-peptide (Sigma) displacement buffer (MENG, 20 mM Na_2MoO_4, 1 mg/ml FLAG peptide). TSDS-PAGE resolved samples were stained using the Silver Stain Plus Kit (Bio-Rad).

Sucrose density gradients

Liver cytosols were made in MENG plus 1X protease inhibitor cocktail buffer as described above, and diluted in the same buffer to a protein concentration of 3.0 mg/ml as

Molecular Pharmacology Fast Forward. Published on September 20, 2006 as DOI: 10.1124/mol.106.029215
This article has not been copyedited and formatted. The final version may differ from this version.

determined by BCA assay (Pierce). Cytosol samples were layered (400 µl/sample) onto 5 ml 10-30% sucrose gradients. Tubes were centrifuged in a Beckman VTI 65.2 vertical rotor at 65,000 rpm for 135 min. Samples were fractionated (200 µl/fraction) using an ISCO model 640 density gradient fractionator. Fractionated proteins were then resolved by TSDS-PAGE using 8% gels followed by transfer onto PVDF membrane. AHR, XAP2, and HSP90 (using anti-HSP84 and anti-HSP86 monoclonal antibodies (Affinity BioReagents)) were visualized as described above. Additionally, ^{125}I-streptavidin bands were quantified by filmless autoradiographic analysis using the Cyclone™ storage phosphor system in conjunction with the OptiQuant™ image analysis software (Perkin Elmer).

AHR immunoprecipitations in Hepa-1 cells versus mouse liver

Hepa-1 cells were maintained at 37°C, 5% CO_2 in alpha modified minimal essential media (Sigma) supplemented with 10% FBS (Hyclone Labs), 1000 Units/ml penicillin, and 0.1 mg/ml streptomycin (Sigma). Hepa-1 cytosol was prepared by homogenizing one confluent 100 mm dish of cells in 1.2 ml of buffer composed of MENG, 20 mM Na_2MoO_4, 0.1% NP-40, and 1X protease inhibitor cocktail using a steel Dounce homogenizer. Mouse liver cytosol was prepared in the same way as described above, except that the buffer used here was the same as was used for making make Hepa-1 cytosol. Homogenates were centrifuged at 100,000 x g for 45 min to isolate cytosol. Immunoprecipitations were performed by incubating 100 µg of cytosol plus 600 µl of homogenization buffer supplemented with 2 mg/ml BSA with 40 µl of anti-rabbit IgG agarose prebound to either non-specific IgG or anti-AHR polyclonal IgG. Samples were

Molecular Pharmacology Fast Forward. Published on September 20, 2006 as DOI: 10.1124/mol.106.029215
This article has not been copyedited and formatted. The final version may differ from this version.

mixed at 4° C for 3 h followed by four washes with homogenization buffer supplemented with 50 mM NaCl. Samples were resolved by TSDS-PAGE and transferred onto PVDF membrane. Immunoblotting and filmless autoradiographic analysis was performed as described above.

Liver cytoplasmic and nuclear extract preparation

Liver (100 mg) was homogenized in 2 ml of MENG plus protease inhibitor cocktail using a steel Dounce homogenizer (20 strokes). The homogenate was spun at 1000 x g for 10 min, after which cytoplasmic extracts were isolated by centrifugation of the supernatant at 100,000 x g for 45 min. The 1000 x g pellet was washed 1X with 2 ml of homogenization buffer plus 0.1% NP-40 followed by a 10 min 1000 x g spin. Nuclear extracts were then isolated by resuspending the 1000 x g pellet in 2 volumes of pellet wash buffer plus 400 mM KCl. The resuspended pellets were periodically vortexed over 10 min followed by centrifugation at 21,000 x g for 30 min. Supernatants from the 21,000 x g spin were collected as the nuclear extract. Protein concentration was determined by BCA assay and samples resolved by TSDS-PAGE. RXRα (antibody, Santa Cruz Biotech) was used as a nuclear marker protein.

Microarray analysis

Total RNA was isolated from wild-type (n=3) and $Tg18^{+/+}$ (n=3) mouse livers by TRI® Reagent, as described above. RNA was further purified with RNeasy kit (Qiagen), according to the manufacturer's protocol. The quality of RNA was confirmed by agarose gel electrophoresis and on Bioanalyzer (Agilent Technologies).

Molecular Pharmacology Fast Forward. Published on September 20, 2006 as DOI: 10.1124/mol.106.029215
This article has not been copyedited and formatted. The final version may differ from this version.

Subsequently, total RNA was labeled using One-Cycle Target Labeling and Control Reagents (Affymetrix) and scanned with GeneChip® Scanner 3000 at the microarray core facility of the Huck Institutes of Life Sciences, Pennsylvania State University. Microarray experiments were performed using the GeneChip® Mouse Genome 430 2.0 arrays comparing transgenic versus wild-type mice (4 week old females).

Raw-data files were subjected to background adjustment, normalization and summarization using RMAexpress (0.3 release, (Irizarry et al., 2003)). Subsequently, the output from RMAexpress was analyzed by Significance Analysis of Microarrays (SAM, Version 2.23A, (Tusher et al., 2001)) with the following selections: 100 permutations, K-nearest neighbors imputer and 10 neighbors. Expression value comparisons were deemed significant at a delta-value of 1.0 and 2-fold change. 36 probe-sets were found to be significant with a false discovery rate of 2 percent (Table 1 & 2). Genes found to be significantly under-expressed in XAP2 transgenic mice were further analyzed by QRT-PCR.

Molecular Pharmacology Fast Forward. Published on September 20, 2006 as DOI: 10.1124/mol.106.029215
This article has not been copyedited and formatted. The final version may differ from this version.

Results

Transgenic mice display enhanced expression of hepatic XAP2 that exists in a complex with the AHR- In the liver the AHR serves to regulate the expression of numerous enzymes involved in endobiotic and xenobiotic metabolism. XAP2 shows considerable variability in protein levels present between tissues, and in liver is relatively low compared with some non-hepatic tissues (Fig. 1A). This raises the question of whether XAP2 is a limiting component in modulating AHR activity in the liver in comparison to some higher expressing tissues, such as spleen, thymus, and brain. To address this transgenic mouse lines were created in the C57BL/6J strain background that resulted in elevated XAP2 expression under the transcriptional control of the mouse transthyretin promoter. Mouse XAP2 cDNA, containing a carboxy-terminal FLAG-tag, was cloned into exon 2 of the TTR1exV3 vector (Fig. 1B) which has been used by numerous labs resulting in transgenic mouse lines that exhibit robust liver-specific expression of exogenous genes (Mallet et al., 2002; Wu et al., 1996). Mice that contained the XAP2-FLAG transgene were identified by a PCR based screen (Fig. 1C) and two founder lines, designated Tg04 and Tg18 were used for subsequent studies.

To confirm that XAP2-FLAG expression was isolated to the liver in the transgenic mouse lines whole cell extracts were prepared using tissues collected from wild-type, $Tg04^{+/+}$, and $Tg18^{+/+}$ animals. In both transgenic lines, but not in wild-type, XAP2-FLAG expression appeared to be present only in the liver of these animals (Fig. 2A). In cell culture and other *in vitro* systems XAP2-FLAG is capable of existing in AHR complexes to the same degree as the normal non-tagged form (Meyer et al., 2000). To validate that it does exist in the unliganded AHR complex in the transgenic mouse

Molecular Pharmacology Fast Forward. Published on September 20, 2006 as DOI: 10.1124/mol.106.029215
This article has not been copyedited and formatted. The final version may differ from this version.

lines FLAG immunoprecipitations were performed using liver cytosols from wild-type, $Tg04^{+/-}$, and $Tg18^{+/-}$ mice. Immunoblot results (Fig. 2B) confirmed that XAP2-FLAG was present in a complex with the AHR and HSP90.

Wild-type and transgenic mice have similar gene expression patterns both basally and following AHR ligand activation- Increased XAP2 expression through exogenous means has been demonstrated to modulate AHR transcriptional activity in cell culture and yeast systems (Carver et al., 1998; Hollingshead et al., 2004; LaPres et al., 2000). The ability of XAP2 to alter AHR transcriptional properties in animal systems, however, has yet to be addressed. To that end male wild-type and transgenic homozygous mice were administered the moderate affinity AHR ligand, β-NF, via intraperitoneal injection for 6 h using a broad range of doses (1×10^{-3} to 2.5×10^{2} mg/kg). We previously reported that XAP2-mediated repression of AHR activity is most pronounced using sub-saturating doses of the moderate affinity AHR ligand iodoflavone (Petrulis et al., 2003). Therefore β-NF was chosen as the ligand for these experiments based on its similarity to iodoflavone, both in structure and AHR-binding affinity. The dose-response curve generated for CYP1A1 mRNA shows no difference in expression levels in wild-type versus both the $Tg04^{+/+}$ and $Tg18^{+/+}$ mouse lines (Fig. 3A). The dose-response relationship of CYP1A1 mRNA levels agrees nicely with the previously reported studies in C57BL/6J mice documenting aryl hydrocarbon hydroxylase activity in response to β-NF treatment (Niwa et al., 1975). Also, it is noteworthy that no differences in CYP1A1 expression were observed between genotypes in females as well (data not shown). The expression levels of other AHR responsive genes were also measured. No difference in

Molecular Pharmacology Fast Forward. Published on September 20, 2006 as DOI: 10.1124/mol.106.029215
This article has not been copyedited and formatted. The final version may differ from this version.

the expression of CYP1A2, UGT1A2, NQO1, CAR, or NRF2 was observed in control samples or samples collected from mice exposed to sub-saturating concentrations (20mg/kg) of β-NF (Fig. 3B-F). In response to a saturating concentration (250 mg/kg) of β-NF statistically different levels of CYP1A2 (reduced) and NQO1 (increased) mRNA were detected. However, it seems unlikely that these modest changes in mRNA would result in a biologically relevant modulation in CYP1A2 or NQO1 protein levels. It should be noted that we have recently identified CAR to be inducible through an AHR-dependent mechanism (manuscript submitted). Because expression of the genes UGT1A2, NQO1, and NRF2 could be induced indirectly by oxidant stress caused by β-NF metabolism we wanted to be sure that their induction was AHR-dependent. As seen in figure 3G, $AHR^{-/-}$ mice showed no increase in UGT1A2, NQO1, or NRF2 showing that their induction by β-NF was through activation of the AHR. As expected CYP1A1 expression was virtually undetectable in $AHR^{-/-}$ mice. Wild-type mice treated in parallel with $AHR^{-/-}$ mice displayed β-NF-induced increases in expression of CYP1A1, UGT1A2, NQO1, and NRF2 (data not shown).

PPARα transcriptional activity is unaltered in wild-type versus transgenic mice- XAP2 also has been shown to attenuate the transcriptional activity of the nuclear receptor PPARα in cell culture systems (Sumanasekera et al., 2003). To see if hepatic PPARα activity was altered in the presence of increased XAP2 levels wild-type and $Tg04^{+/+}$ mice were administered the PPARα-specific ligand WY-14,643 via gavage. The mRNA levels of two PPARα responsive genes, ACOX1 and FABPL, were efficiently induced in WY-14,643 treated mice. However, no differences in mRNA amounts were observed between

Molecular Pharmacology Fast Forward. Published on September 20, 2006 as DOI: 10.1124/mol.106.029215
This article has not been copyedited and formatted. The final version may differ from this version.

wild-type and Tg04$^{+/+}$ mice in control or ligand-induced samples (Fig. 4). It appears as though increased XAP2 expression in the liver exerts no effects on PPARα transcriptional activity.

Stoichiometric binding of XAP2 in the AHR complex is similar in wild-type and transgenic mice- Since AHR transcriptional capacity appears to be unaltered by the enhanced expression of XAP2 we desired to see if XAP2 occupancy in the cytosolic AHR complex was changed. First, sucrose density fractionation of wild-type and Tg18$^{+/+}$ liver cytosol was performed and samples were resolved by TSDS-PAGE. Immunoblot detection of AHR, HSP90, and XAP2 was performed using ^{125}I-streptavidin and bands were quantified by filmless autoradiographic analysis. Although Tg18$^{+/+}$ samples show a broader XAP2 elution profile than wild-type samples, enrichment of XAP2 in the AHR positive fractions is not observed (Fig. 5A). Most cellular XAP2 appears to exist in small complexes or as a monomer. This implies that XAP2 presence in the AHR complex may be the same between wild-type and transgenic animals. To distinguish with certainty if this is indeed correct AHR immunoprecipitations were performed and the amount of XAP2 co-precipitated with the receptor was assessed. As suspected, little difference in co-precipitated XAP2 was observed in wild-type versus hemi- and homozygous transgenic animals (Fig. 5B), even given the large increase in XAP2 expression in the transgenic lines (Fig. 5B, Inputs). Filmless autoradiographic analysis quantification of XAP2 co-adsorbed with the AHR demonstrated that no increase (hemizygous) or less than a 2-fold increase (homozygous) of XAP2 was present in transgenic AHR complexes (data not shown). Taken together, these results would lead to the conclusion that normal

Molecular Pharmacology Fast Forward. Published on September 20, 2006 as DOI: 10.1124/mol.106.029215
This article has not been copyedited and formatted. The final version may differ from this version.

liver expression of XAP2, although low relative to some non-hepatic tissues, is sufficient to obtain maximal occupancy in AHR complexes.

AHR complexes in Hepa-1 cells and mouse liver are saturated with XAP2- Contrary to a previous report which concluded that, in Hepa-1 cells, XAP2 is present in ~40% of AHR complexes (Petrulis et al., 2000), a recent study using these cells determined that AHR complexes are completely saturated with XAP2 (Pollenz et al. 2006). Since hepatic AHR complexes in mouse liver also appear to be maximally associated with XAP2 we wanted to assess the relative levels of AHR and XAP2 between the two. As seen in figure 6A, the levels of the AHR (3-fold) and XAP2 (4-fold) are elevated in Hepa-1 cells as compared to mouse liver. Immunoprecipitation of the AHR from Hepa-1 and liver cytosols results in an equal proportion of XAP2 co-adsorption relative to the amount of AHR precipitated. The results from this experiment further support that the AHR in Hepa-1 and mouse liver cytosols is maximally bound with XAP2.

AHR in wild-type and transgenic livers is predominantly localized in the cytoplasm- XAP2 is known to cause cytoplasmic sequestration of the AHR in cell culture systems (Petrulis et al., 2000). To determine if AHR cellular localization is altered in transgenic as compared to wild-type mice cytoplasmic and nuclear extracts were prepared from wild-type and $Tg04^{+/-}$ mouse livers. Immunoblot analysis reveals that in wild-type mice AHR is localized almost exclusively in the cytoplasm with only a minor fraction being found in the nucleus (Fig. 6B). RXRα was used as a positive control for

Molecular Pharmacology Fast Forward. Published on September 20, 2006 as DOI: 10.1124/mol.106.029215
This article has not been copyedited and formatted. The final version may differ from this version.

constitutively nuclear localization. In transgenic samples the AHR shows identical cellular distribution as found in wild-type samples. In addition, XAP2 is found to be predominantly cytoplasmic in wild-type and transgenic liver samples with some nuclear localization.

Transgenic XAP2 binds to HSP90 in high abundance- In order to determine if XAP2 binds to any previously unidentified cytosolic proteins transgenic XAP2 was immunoprecipitated with anti-FLAG resin. Adsorbed XAP2-FLAG complexes were eluted off the resin, and TSDS-PAGE resolved samples were visualized by silver stain procedure. Two approximately 90 kDa proteins were found to co-adsorb with XAP2-FLAG, and are likely isoforms of HSP90 (Fig. 7). AHR co-immunoprecipitation can not be determined due to the nonspecific 97kDa band that is found to migrate at the same molecular weight as the AHR. No other high abundance interactions with XAP2 were observed implying that XAP2 may exist largely as a monomer or bound to HSP90, which is in agreement with the sucrose density gradient studies (Fig. 5A).

The identification of genes whose expression is altered by elevated XAP2 levels- Gene expression studies were performed using the Affymetrix GeneChip® Mouse Genome 430 2.0 arrays in an attempt to identify previously uncharacterized XAP2-regulated genes. Probe-sets that displayed a two-fold or greater difference in expression (see methods section for details of data analysis) between genotypes are shown in Tables 1 and 2. As expected, XAP2 shows the largest difference in expression between wild-type and $Tg18^{+/+}$ samples. Most of the probe-sets that show elevated expression (Table

1) in transgenic as compared to wild-type samples do not represent well-defined genes making it difficult to speculate how XAP2 might serve to modulate their function. Interestingly, mRNA expression of the Phase I CYP3A41, and 2B20 enzymes and the Phase II enzyme SULT3A1 are repressed in transgenic samples (Table 2). Additionally, a number of other genes encoding functionally dissimilar enzymes are repressed in transgenic mice livers. Differential mRNA expression for a subset of array targets was verified using QRT-PCR, and genes that were confirmed to be dissimilar between genotypes are indicated in Table 2 by an asterisk. In the future it will be of interest to see which of the genes are indeed genuinely regulated by XAP2, and how their function can be altered through XAP2-mediated modulation.

Molecular Pharmacology Fast Forward. Published on September 20, 2006 as DOI: 10.1124/mol.106.029215
This article has not been copyedited and formatted. The final version may differ from this version.

Discussion

As mentioned previously, the AHR regulates the expression of a number of genes involved in the metabolic clearance of exogenous compounds. This seemingly benign biological role the AHR plays in metabolism is in opposition to the toxic endpoints, which occur in response to prolonged AHR transcriptional activity, such as hepatomegaly (Fernandez-Salguero et al., 1996) and hepatocarcinogenesis (Moennikes et al., 2004). Because of the delicate interplay between physiologic and toxic endpoints mediated through AHR activity, it is necessary to obtain a better mechanistic understanding of AHR regulation. Earlier studies have shown that AHR transcriptional control is modulated by the AHR oligomeric complex chaperone proteins HSP90 and XAP2. Since overall XAP2 levels are highly variable between tissues relative to HSP90 (Fig. 1A) it was considered that differential expression of XAP2 may perhaps serve as a mechanism to regulate AHR activity between tissues. If indeed XAP2 does modulate AHR differently between tissues then it is possible that the XAP2 levels within a tissue could enhance or attenuate the susceptibility of individual tissues to AHR-mediated toxicity.

The creation of transgenic mouse lines under the transcriptional control of the mouse transthyretin promoter resulted in founder lines that contained liver-specific XAP2 expression in levels greater than any other tissue examined (data not shown). Given this large increase in hepatic XAP2, it was quite surprising that AHR transcriptional output was observed to be virtually identical between wild-type and transgenic mouse lines (Fig. 3). We previously noted that XAP2-mediated repression of AHR activity was most pronounced at sub-saturating levels of AHR ligand (Petrulis et al., 2003). Therefore, the mRNA levels for numerous metabolic (CYP1A1, CYP1A2, NQO1, and UGT1A2) or

metabolically relevant (CAR and NRF2) genes were examined at saturating (100 and 250 mg/kg) and sub-saturating (<100 mg/kg) amounts of the AHR ligand, β-NF. At all doses examined gene expression was virtually unchanged between genotypes. NRF2 has recently been demonstrated to be an AHR-inducible gene (reviewed in (Kohle and Bock, 2006)). Because NRF2 also regulates the transcription of numerous Phase II enzymes, it is possible that the elevated expression of NQO1 and UGT1A2 observed here following β-NF treatment is due to the combinatorial regulation of these genes by the AHR and NRF2. In addition, transcriptional activity of PPARα was unaltered between genotypes (Fig. 4) unlike what has been observed in cell culture (Sumanasekera et al., 2003). Further work must be done to mechanistically explain discrepancies between the cell culture and *in vivo* reports of XAP2's ability to attenuate PPARα activity. Despite these negative results the microarray data suggests that enhanced XAP2 expression is capable of influencing gene expression. It should be noted that two pathologists observed no significant morphological differences between wild-type and transgenic formalin-fixed liver sections prepared from 2, 4, and 6 week old mice.

In order to mechanistically explain why AHR transcriptional properties were unaltered we examined relative levels of HSP90 and XAP2 in the unliganded AHR complex. Sucrose density gradient fractionation and immunoprecipitation experiments (Fig. 5 & 6A) highlighted that most XAP2 in wild-type animals is not bound along with the AHR. Furthermore, increasing the amount of XAP2 available for binding in transgenic animals resulted in no appreciable increase in the stoichiometric binding of XAP2 in the AHR complex. This result was surprising considering that a previous stoichiometric evaluation of AHR complexes in Hepa-1 cells found that only ~40% of

Molecular Pharmacology Fast Forward. Published on September 20, 2006 as DOI: 10.1124/mol.106.029215
This article has not been copyedited and formatted. The final version may differ from this version.

cytosolic AHR is bound to XAP2 (Petrulis et al., 2000). However, a recent report has questioned this finding suggesting that, in Hepa-1 cells, AHR complexes are endogenously saturated with XAP2 (Pollenz et al., 2006). The results presented in figure 6A show that the AHR in Hepa-1 cells and wild-type liver cytosol binds to XAP2 with the same stoichiometry. This finding provides strong support for the idea that the cytosolic hepatic AHR is maximally complexed with the AHR. Additionally, experiments performed using *in vitro* translated AHR and XAP2 demonstrated that XAP2 has a high affinity for the AHR, and that complete association of XAP2 with the AHR occurred following the mixing-together of individually translated components (Meyer et al., 1998). XAP2 expression is lower in liver than in many other tissues (Fig. 1A), yet XAP2 appears to be present in excess molar quantities compared to the AHR. Therefore, XAP2 in all probability does not regulate AHR function in various tissues by means of its differential expression. Taken together, it would appear as though that the endogenous levels of XAP2 in mouse liver are more than sufficient to allow for maximal formation of AHR-HSP90-XAP2 complexes.

Previous cell culture studies have demonstrated the ability of XAP2 to stabilize the AHR, resulting in increased cytosolic levels and elevated AHR transcriptional activity (Kazlauskas et al., 2000; LaPres et al., 2000; Lees et al., 2003). AHR complexes isolated from Hepa-1 cells and wild-type mouse liver are each maximally associated with XAP2. Unlike Hepa-1 cells, however, the increased expression of XAP2 *in vivo* does not result in the elevation of total cytosolic AHR levels. AHR levels in transgenic animals were consistently found to be identical to wild-type mice (Fig. 2B, 5B, and 6B), and therefore it appears as though the stabilization of the AHR and enhanced transcriptional activity

that occurs in cell culture following increased XAP2 expression is an artifact of the experimental system used. This conclusion is supported by a recent report that showed only a modest decrease in AHR levels following the knock-down of XAP2 expression in Hepa-1 cells (Pollenz et al., 2005). It is also possible that since hepatocytes *in vivo* are fundamentally different then cells grown on plastic culture dishes that some other factors regulate AHR function *in vivo* that have yet to be discovered.

XAP2-mediated repression of AHR activity in cell culture has been speculated to result from its ability to sequester the AHR in the cytoplasm and displace p23 from the AHR complex (Hollingshead et al., 2004). *In vivo*, however, the AHR appears to normally be exclusively cytoplasmic in wild-type animals with no change in cellular localization in transgenic lines. Incorporation of p23 in the AHR complex *in vivo* could not be detected (data not shown). It is likely that since the AHR is maximally bound to XAP2 *in vivo*, XAP2 is responsible for the cytoplasmic localization of the AHR. If this is indeed true then XAP2 may play a critical role in regulating AHR function that cannot be addressed using the transgenic model presented in this study. The creation of XAP2 null mice will address if this regulatory mechanism occurs *in vivo*.

Epidemiological studies in human populations have shown inter-individual variability in AHR ligand-binding affinity and CYP1 inducibility which cannot be explained by AHR polymorphisms (Nebert et al., 2004). Therefore, it is possible that differential expression of chaperone proteins such as HSP90, XAP2, and p23 could play a role in some of these observed variability's. Consequently, the information collected in this study is useful in that it appears to suggest that inter-individual differences in AHR

activity are not mediated through varying XAP2 levels. However, the total absence of XAP2 expression may influence AHR activity.

Experiments carried out in order to determine whether XAP2 binds to any previously unidentified cytosolic proteins identified no new protein interactions (Fig. 7A). These results by no means conclude that XAP2 does not bind other unidentified proteins, as other non-AHR complex interactions have already been characterized, but it suggests that additional high abundance interactions do not exist among soluble proteins in the liver. We also provide a list of genes that were differentially regulated in wild-type and transgenic animals. Future studies will determine if any of these genes are regulated by the endogenous XAP2 normally found at low levels in mouse liver, or if their altered expression is simply due to the enhanced expression of XAP2 in these transgenic lines.

It is evident from this report that hepatic XAP2 is not limiting within the context of AHR complexes as hypothesized. Future work using XAP2 null mouse lines needs to be performed to determine what kind of role the endogenous pool of XAP2 plays in modulating AHR function. It will be of interest to note whether XAP2 is saturating in its ability regulate hepatic AHR activity, as inferred from this work, or whether XAP2 is completely non-essential in the context of regulating the hepatic AHR. Additionally, whether XAP2 modulates non-hepatic development of AHR-mediated phenotypes, such as the endothelial cell-mediated vascular defect in the fetal liver (Walisser et al., 2005) may be of interest to explore in the future.

Acknowledgements

We would like to thank Dr. Terry Van Dyke (University of North Carolina) for the TTR1exV3 vector used to create the transgenic mouse lines. We would also like to thank Dr. Mary Kennett and Dr. Arthur Hattel for histological examination of tissue sections. Finally, we would like to thank Dr. Christopher Bradfield and Ed Glover for providing $AHR^{-/-}$ mice.

References

Andreola F, Calvisi DF, Elizondo G, Jakowlew SB, Mariano J, Gonzalez FJ and De Luca LM (2004) Reversal of liver fibrosis in aryl hydrocarbon receptor null mice by dietary vitamin A depletion. *Hepatology* **39**(1):157-166.

Baba T, Mimura J, Nakamura N, Harada N, Yamamoto M, Morohashi K and Fujii-Kuriyama Y (2005) Intrinsic function of the aryl hydrocarbon (dioxin) receptor as a key factor in female reproduction. *Mol Cell Biol* **25**(22):10040-10051.

Carver LA and Bradfield CA (1997) Ligand-dependent interaction of the aryl hydrocarbon receptor with a novel immunophilin homolog in vivo. *J Biol Chem* **272**(17):11452-11456.

Carver LA, Jackiw V and Bradfield CA (1994) The 90-kDa heat shock protein is essential for Ah receptor signaling in a yeast expression system. *J Biol Chem* **269**(48):30109-30112.

Carver LA, LaPres JJ, Jain S, Dunham EE and Bradfield CA (1998) Characterization of the Ah receptor-associated protein, ARA9. *J Biol Chem* **273**(50):33580-33587.

Chen HS and Perdew GH (1994) Subunit composition of the heteromeric cytosolic aryl hydrocarbon receptor complex. *J Biol Chem* **269**(44):27554-27558.

Fernandez-Salguero P, Pineau T, Hilbert DM, McPhail T, Lee SS, Kimura S, Nebert DW, Rudikoff S, Ward JM and Gonzalez FJ (1995) Immune system impairment and hepatic fibrosis in mice lacking the dioxin-binding Ah receptor. *Science* **268**(5211):722-726.

Fernandez-Salguero PM, Hilbert DM, Rudikoff S, Ward JM and Gonzalez FJ (1996) Aryl-hydrocarbon receptor-deficient mice are resistant to 2,3,7,8-tetrachlorodibenzo-p-dioxin-induced toxicity. *Toxicol Appl Pharmacol* **140**(1):173-179.

Fernandez-Salguero PM, Ward JM, Sundberg JP and Gonzalez FJ (1997) Lesions of aryl-hydrocarbon receptor-deficient mice. *Vet Pathol* **34**(6):605-614.

Hollingshead BD, Petrulis JR and Perdew GH (2004) The aryl hydrocarbon (Ah) receptor transcriptional regulator hepatitis B virus X-associated protein 2 antagonizes p23 binding to Ah receptor-Hsp90 complexes and is dispensable for receptor function. *J Biol Chem* **279**(44):45652-45661.

Irizarry RA, Bolstad BM, Collin F, Cope LM, Hobbs B and Speed TP (2003) Summaries of Affymetrix GeneChip probe level data. *Nucleic Acids Res* **31**(4):e15.

Kazlauskas A, Poellinger L and Pongratz I (1999) Evidence that the co-chaperone p23 regulates ligand responsiveness of the dioxin (Aryl hydrocarbon) receptor. *J Biol Chem* **274**(19):13519-13524.

Kazlauskas A, Poellinger L and Pongratz I (2000) The immunophilin-like protein XAP2 regulates ubiquitination and subcellular localization of the dioxin receptor. *J Biol Chem* **275**(52):41317-41324.

Kewley RJ, Whitelaw ML and Chapman-Smith A (2004) The mammalian basic helix-loop-helix/PAS family of transcriptional regulators. *Int J Biochem Cell Biol* **36**(2):189-204.

Kohle C and Bock KW (2006) Activation of coupled Ah receptor and Nrf2 gene batteries by dietary phytochemicals in relation to chemoprevention. *Biochem Pharmacol*.

Lahvis GP, Lindell SL, Thomas RS, McCuskey RS, Murphy C, Glover E, Bentz M, Southard J and Bradfield CA (2000) Portosystemic shunting and persistent fetal vascular structures in aryl hydrocarbon receptor-deficient mice. *Proc Natl Acad Sci U S A* **97**(19):10442-10447.

LaPres JJ, Glover E, Dunham EE, Bunger MK and Bradfield CA (2000) ARA9 modifies agonist signaling through an increase in cytosolic aryl hydrocarbon receptor. *J Biol Chem* **275**(9):6153-6159.

Lees MJ, Peet DJ and Whitelaw ML (2003) Defining the role for XAP2 in stabilization of the dioxin receptor. *J Biol Chem* **278**(38):35878-35888.

Ma Q and Whitlock JP, Jr. (1997) A novel cytoplasmic protein that interacts with the Ah receptor, contains tetratricopeptide repeat motifs, and augments the transcriptional response to 2,3,7,8-tetrachlorodibenzo-p-dioxin. *J Biol Chem* **272**(14):8878-8884.

Mallet VO, Mitchell C, Guidotti JE, Jaffray P, Fabre M, Spencer D, Arnoult D, Kahn A and Gilgenkrantz H (2002) Conditional cell ablation by tight control of caspase-3 dimerization in transgenic mice. *Nat Biotechnol* **20**(12):1234-1239.

Meyer BK, Petrulis JR and Perdew GH (2000) Aryl hydrocarbon (Ah) receptor levels are selectively modulated by hsp90-associated immunophilin homolog XAP2. *Cell Stress Chaperones* **5**(3):243-254.

Meyer BK, Pray-Grant MG, Vanden Heuvel JP and Perdew GH (1998) Hepatitis B virus X-associated protein 2 is a subunit of the unliganded aryl hydrocarbon receptor core complex and exhibits transcriptional enhancer activity. *Mol Cell Biol* **18**(2):978-988.

Moennikes O, Loeppen S, Buchmann A, Andersson P, Ittrich C, Poellinger L and Schwarz M (2004) A constitutively active dioxin/aryl hydrocarbon receptor promotes hepatocarcinogenesis in mice. *Cancer Res* **64**(14):4707-4710.

Nair SC, Toran EJ, Rimerman RA, Hjermstad S, Smithgall TE and Smith DF (1996) A pathway of multi-chaperone interactions common to diverse regulatory proteins: estrogen receptor, Fes tyrosine kinase, heat shock transcription factor Hsf1, and the aryl hydrocarbon receptor. *Cell Stress Chaperones* **1**(4):237-250.

Nebert DW, Dalton TP, Okey AB and Gonzalez FJ (2004) Role of aryl hydrocarbon receptor-mediated induction of the CYP1 enzymes in environmental toxicity and cancer. *J Biol Chem* **279**(23):23847-23850.

Nebert DW, Roe AL, Dieter MZ, Solis WA, Yang Y and Dalton TP (2000) Role of the aromatic hydrocarbon receptor and [Ah] gene battery in the oxidative stress response, cell cycle control, and apoptosis. *Biochem Pharmacol* **59**(1):65-85.

Niwa A, Kumaki K, Nebert DW and Poland AP (1975) Genetic expression of aryl hydrocarbon hydroxylase activity in the mouse. Distinction between the "responsive" homozygote and heterozygote at the Ah locus. *Arch Biochem Biophys* **166**(2):559-564.

Panda S, Hogenesch JB and Kay SA (2002) Circadian rhythms from flies to human. *Nature* **417**(6886):329-335.

Petrulis J and Perdew G (2002) The role of chaperone proteins in the aryl hydrocarbon receptor core complex. *Chem Biol Interact* **141**(1-2):25.

Petrulis JR, Hord NG and Perdew GH (2000) Subcellular localization of the aryl hydrocarbon receptor is modulated by the immunophilin homolog hepatitis B virus X-associated protein 2. *J Biol Chem* **275**(48):37448-37453.

Petrulis JR, Kusnadi A, Ramadoss P, Hollingshead B and Perdew GH (2003) The hsp90 Co-chaperone XAP2 alters importin beta recognition of the bipartite nuclear localization signal of the Ah receptor and represses transcriptional activity. *J Biol Chem* **278**(4):2677-2685.

Pollenz RS and Dougherty EJ (2005) Redefining the role of the endogenous XAP2 and C-terminal hsp70-interacting protein on the endogenous Ah receptors expressed in mouse and rat cell lines. *J Biol Chem* **280**(39):33346-33356.

Pollenz RS, Wilson SE and Dougherty EJ (2006) Role of endogenous XAP2 protein on the localization and nucleocytoplasmic shuttling of the endogenous mouse Ahb-1 receptor in the presence and absence of ligand. *Mol Pharmacol*.

Pongratz I, Mason GG and Poellinger L (1992) Dual roles of the 90-kDa heat shock protein hsp90 in modulating functional activities of the dioxin receptor. Evidence that the dioxin receptor functionally belongs to a subclass of nuclear receptors which require hsp90 both for ligand binding activity and repression of intrinsic DNA binding activity. *J Biol Chem* **267**(19):13728-13734.

Schmidt JV, Su GH, Reddy JK, Simon MC and Bradfield CA (1996) Characterization of a murine Ahr null allele: involvement of the Ah receptor in hepatic growth and development. *Proc Natl Acad Sci U S A* **93**(13):6731-6736.

Sumanasekera WK, Tien ES, Turpey R, Vanden Heuvel JP and Perdew GH (2003) Evidence that peroxisome proliferator-activated receptor alpha is complexed with the 90-kDa heat shock protein and the hepatitis virus B X-associated protein 2. *J Biol Chem* **278**(7):4467-4473. Epub 2002 Dec 4413.

Tusher VG, Tibshirani R and Chu G (2001) Significance analysis of microarrays applied to the ionizing radiation response. *Proc Natl Acad Sci U S A* **98**(9):5116-5121.

Walisser JA, Bunger MK, Glover E and Bradfield CA (2004) Gestational exposure of Ahr and Arnt hypomorphs to dioxin rescues vascular development. *Proc Natl Acad Sci U S A* **101**(47):16677-16682.

Walisser JA, Glover E, Pande K, Liss AL and Bradfield CA (2005) Aryl hydrocarbon receptor-dependent liver development and hepatotoxicity are mediated by different cell types. *Proc Natl Acad Sci U S A* **102**(49):17858-17863.

Wu H, Wade M, Krall L, Grisham J, Xiong Y and Van Dyke T (1996) Targeted in vivo expression of the cyclin-dependent kinase inhibitor p21 halts hepatocyte cell-cycle progression, postnatal liver development and regeneration. *Genes Dev* **10**(3):245-260.

Footnotes

This work was supported by NIEHS, National Institutes of Health Grants (ES04869 and ES007799), and the Penn State Transgenic Mouse Facility and NCRR Facilities Improvement Grant 1 CO6 RR14520 (OSP #69310). Portions of this work were presented at the 4th Annual Merck Graduate Student Drug Metabolism Symposium (2006).

Reprint requests: Gary H. Perdew, The Center for Molecular Toxicology and Carcinogenesis, 309 Life Sciences Building, The Pennsylvania State University, University Park, PA 16802, telephone: (814) 865-0400, fax: (814) 863-1696, e-mail: ghp2@psu.edu

Molecular Pharmacology Fast Forward. Published on September 20, 2006 as DOI: 10.1124/mol.106.029215
This article has not been copyedited and formatted. The final version may differ from this version.

Figure Legends

Figure 1. Tissue distribution of XAP2 expression, and XAP2 transgenic mouse production. (A) Various tissues were isolated and cytosol was prepared from two mature male C57BL/6J mice. Immunoblotting was performed to assess XAP2 levels present in these tissues. (B) An illustration of the TTR1ExV3 vector used to create the transgenic mouse lines and the location (exon 2) that the XAP2-FLAG cDNA was inserted. Arrows found below the XAP2-FLAG sequence represent the location of the primer sets used to screen for transgenic animals. Note that the illustration is not drawn to scale. (C) A representative PCR screen used to discriminate between transgenic and wild-type mice.

Figure 2. Transgenic XAP2 expression is localized to the liver and is found in a complex with the AHR. (A) A variety of tissues were isolated and cytosol was prepared from male wild-type, $Tg04^{+/+}$, and $Tg18^{+/+}$ mice. The expression of the XAP2-FLAG transprotein was assessed by immunoblotting using an anti-FLAG antibody. No expression of XAP2-FLAG could be found in any of the non-hepatic tissues examined. (B) Immunoprecipitations of XAP2-FLAG were preformed using liver cytosol made from wild-type, $Tg04^{+/-}$, and $Tg18^{+/-}$ mice. Immunoblotting confirmed that XAP2-FLAG is capable of existing in a complex with the AHR and HSP90.

Figure 3. AHR regulation of target genes is unaltered in wild-type versus transgenic mice upon exposure to non-saturating and saturating concentrations of an AHR ligand.

Molecular Pharmacology Fast Forward. Published on September 20, 2006 as DOI: 10.1124/mol.106.029215
This article has not been copyedited and formatted. The final version may differ from this version.

Male mice between six and ten weeks of age were injected intraperitoneally with various concentrations of β-NF (10^{-3} to 2.5 x 10^{2} mg/kg) or corn oil vehicle for 6 h. QRT-PCR was used to quantify mRNA expression of selected genes. (A) A full dose-response curve of CYP1A1 expression was generated observing no change in CYP1A1 mRNA content between genotypes at any β-NF dose. The expression levels of (B) CYP1A2, (C) UGT1A2, (D) NQO1, (E) CAR, and (F) NRF2 mRNA were also unchanged between genotypes in control and β-NF treated (20 mg/kg and 250 mg/kg) samples. The number of animals used for each treatment group (n=8) except β-NF concentrations of 1.0 and 2.5 x 10^{2} mg/kg (n=4). (G) $AHR^{-/-}$ mice (n=3) were injected intraperitoneally with 50 mg/kg β-NF or corn oil for 5 h. All values shown are normalized relative to GAPDH levels. Data presented are mean values, and error bars represent (A) standard error, or (B-G) standard deviation of those samples. (*, **, *** means $p \leq 0.05$, 0.01, or 0.001 respectively)

Figure 4. PPARα regulated gene expression is unaltered between wild-type and transgenic mice in the presence and absence of WY-14,643 treatment. Wild-type or $Tg04^{+/+}$ males were left untreated (n=3) or administered the PPARα specific ligand WY-14,643 (n=6) or corn oil vehicle (n=3) via gavage and livers removed after 7 h. QRT-PCR was used to quantify mRNA levels of (A) ACOX1 and (B) FABPL. No statistical difference was observed between mRNA levels in wild-type versus $Tg04^{+/+}$ mice. All values shown are normalized relative to GAPDH levels. Data presented are mean values, and error bars represent standard deviation of those samples.

Molecular Pharmacology Fast Forward. Published on September 20, 2006 as DOI: 10.1124/mol.106.029215
This article has not been copyedited and formatted. The final version may differ from this version.

Figure 5. The presence of XAP2 in AHR complexes is stoichiometrically similar between wild-type and transgenic mice. (A) Liver cytosol samples (1.2 mg per sample) from wild-type and $Tg18^{+/+}$ mice were fractionated on 10-30% sucrose gradients. Aliquots from each fraction were resolved by TSDS-PAGE and visualized by immunoblot using biotin-conjugated secondary antibodies in combination with ^{125}I-streptavidin. Respective protein bands were quantified by filmless autoradiographic analysis. Diamonds and triangles represent data values obtained for wild-type and $Tg18^{+/+}$ samples, respectively. (B) AHR immunoprecipitations of liver cytosol samples from wild-type and transgenic (hemizygous and homozygous) mice were performed. TSDS-PAGE resolved samples were visualized by immunoblot using biotin-conjugated secondary antibodies in combination with ^{125}I-streptavidin.

Figure 6. The assessment of AHR-XAP2 complex stoichiometry in cell culture versus in liver, and the cellular localization of the AHR in wild-type and transgenic mice. (A) AHR immunoprecipitations were performed using Hepa-1 or wild-type mouse liver cytosol isolated from two animals. TSDS-PAGE resolved samples were visualized by immunoblot using biotin-conjugated secondary antibodies in combination with ^{125}I-streptavidin. The intensity of radiolabeled bands corresponding to the AHR and XAP2 was quantified by filmless autoradiographic analysis. Numerical values shown beneath the bands are representative of the amount of the AHR precipitated or XAP2 co-precipitated in each sample relative to the highest intensity band. (B) Cytoplasmic and nuclear extracts were prepared from livers of wild-type and $Tg04^{+/-}$ mice. Equal amounts of cytoplasmic and nuclear protein were resolve by TSDS-PAGE and samples were

visualized by immunoblot using biotin-conjugated secondary antibodies in combination with ^{125}I-streptavidin. RXRα was used a nuclear marker protein.

Figure 7. Screen for novel XAP2-interacting proteins. XAP2-FLAG was immunoprecipitated from wild-type and Tg18$^{+/+}$ liver cytosol. Adsorbed complexes were eluted off the anti-FLAG resin samples were resolved by TSDS-PAGE followed by protein visualization by silver stain. Asterisk indicates specific XAP2-interacting proteins at ~90 kDa, likely HSP90.

Molecular Pharmacology Fast Forward. Published on September 20, 2006 as DOI: 10.1124/mol.106.029215
This article has not been copyedited and formatted. The final version may differ from this version.

Table 1. Genes that showed increased expression in transgenic versus wild-type mice.

Affymetrix Probe Id	Gene Symbol	Gene Title	Fold Change
1423128_at	Aip	aryl-hydrocarbon receptor-interacting protein	39.5
1448194_a_at	H19	H19 fetal liver mRNA	13.5
1438617_at	---	---	6.2
1451612_at	---	---	3.4
1433837_at	8430408G22Rik	RIKEN cDNA 8430408G22 gene	3.1
1448510_at	Efna1	ephrin A1	2.9
1416895_at	Efna1	ephrin A1	2.8
1435872_at	---	---	2.7
1438519_at	4930429H24Rik	RIKEN cDNA 4930429H24 gene	2.6
1431240_at	Clrf	C-type lectin related f	2.5
1439331_at	4932439E07Rik	RIKEN cDNA 4932439E07 gene	2.4
1453145_at	4933439C20Rik	RIKEN cDNA 4933439C20 gene	2.2
1433836_a_at	8430408G22Rik	RIKEN cDNA 8430408G22 gene	2.2
1420699_at	Clecsf12	C-type (calcium dependent, carbohydrate recognition domain) lectin, superfamily member 12	2.2
1429900_at	5330406M23Rik	RIKEN cDNA 5330406M23 gene	2.2
1435458_at	Pim1	proviral integration site 1	2.1
1426208_x_at	Plagl1	pleiomorphic adenoma gene-like 1	2.1
1440311_at	Sorbs1	Sorbin and SH3 domain containing 1	2.0

Molecular Pharmacology Fast Forward. Published on September 20, 2006 as DOI: 10.1124/mol.106.029215
This article has not been copyedited and formatted. The final version may differ from this version.

Table 2. Genes that showed decreased expression in transgenic versus wild-type mice. Asterisk denotes the genes that were confirmed by QRT-PCR to be different between genotypes.

Affymetrix Probe Id	Gene Symbol	Gene Title	Fold Change
1425837_a_at	Ccrn4l	CCR4 carbon catabolite repression 4-like (S. cerevisiae)	5.3 **(*)**
1421669_at	Sult3a1	sulfotransferase family 3A, member 1	4.3 **(*)**
1428223_at	1700018O18Rik	RIKEN cDNA 1700018O18 gene	3.9 **(*)**
1419136_at	Akr1c18	aldo-keto reductase family 1, member C18	3.4 **(*)**
1419704_at	Cyp3a41	cytochrome P450, family 3, subfamily a, polypeptide 41	2.7 **(*)**
1418028_at	Dct	dopachrome tautomerase	2.7 **(*)**
1440921_at	---	---	2.6
1418025_at	Bhlhb2	basic helix-loop-helix domain containing, class B2	2.4 **(*)**
1422257_s_at	Cyp2b20 /// Cyp2b10	cytochrome P450, family 2, subfamily b, polypeptide 20 /// cytochrome P450, family 2, subfamily b, polypeptide 10	2.4
1425645_s_at	Cyp2b20 /// Cyp2b10	cytochrome P450, family 2, subfamily b, polypeptide 20 /// cytochrome P450, family 2, subfamily b, polypeptide 10	2.3
1445641_at	---	---	2.3
1429169_at	Rbm3	RNA binding motif protein 3	2.2
1451787_at	Cyp2b20	cytochrome P450, family 2, subfamily b, polypeptide 20	2.2
1434449_at	Aqp4	aquaporin 4	2.2
1435595_at	1810011O10Rik	RIKEN cDNA 1810011O10 gene	2.1
1438035_at	AW061290	expressed sequence AW061290	2.1
1420772_a_at	Dsip1	delta sleep inducing peptide, immunoreactor	2.0 **(*)**
1415834_at	Dusp6	dual specificity phosphatase 6	2.0 **(*)**

Molecular Pharmacology Fast Forward. Published on September 20, 2006 as DOI: 10.1124/mol.106.029215
This article has not been copyedited and formatted. The final version may differ from this version.

Figure 1

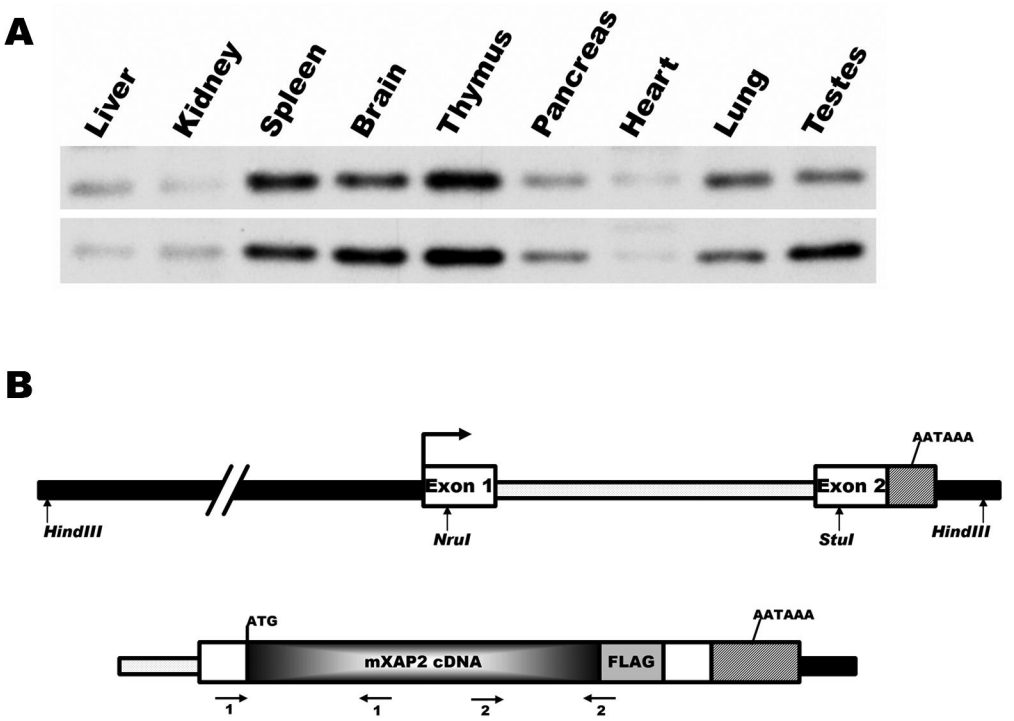

Molecular Pharmacology Fast Forward. Published on September 20, 2006 as DOI: 10.1124/mol.106.029215
This article has not been copyedited and formatted. The final version may differ from this version.

Figure 2

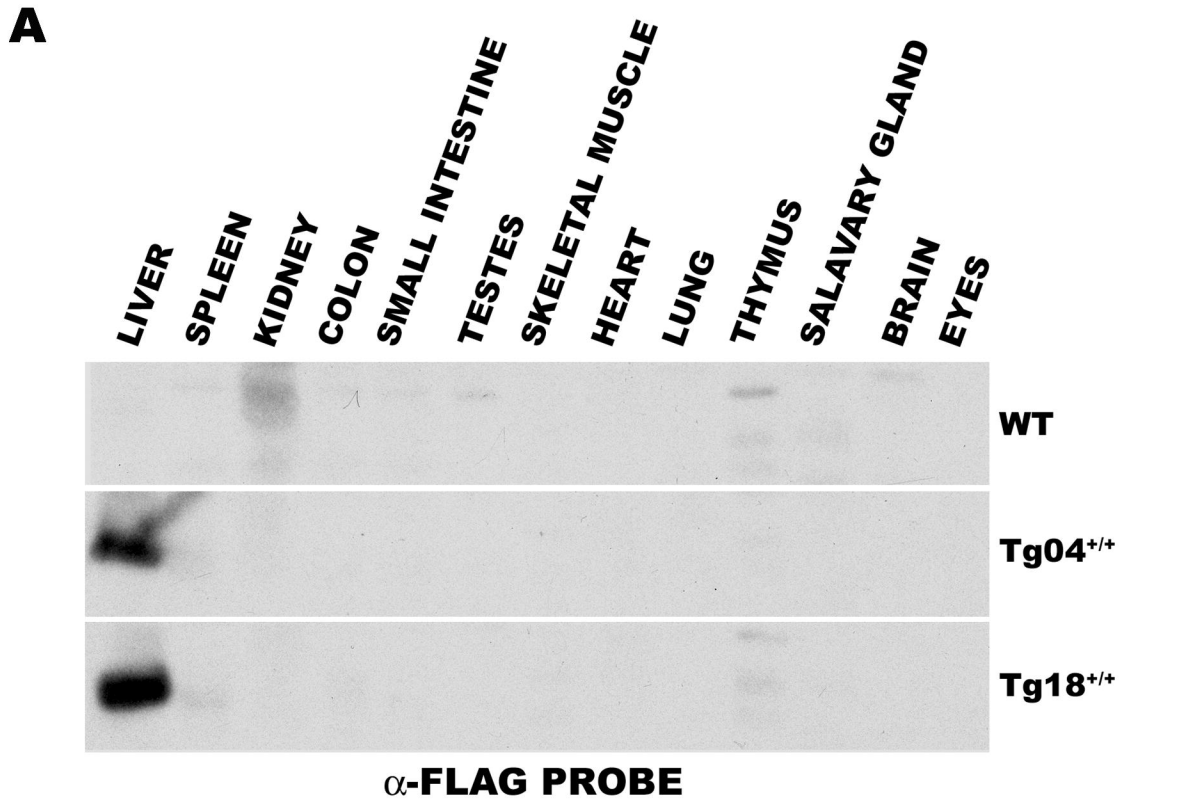

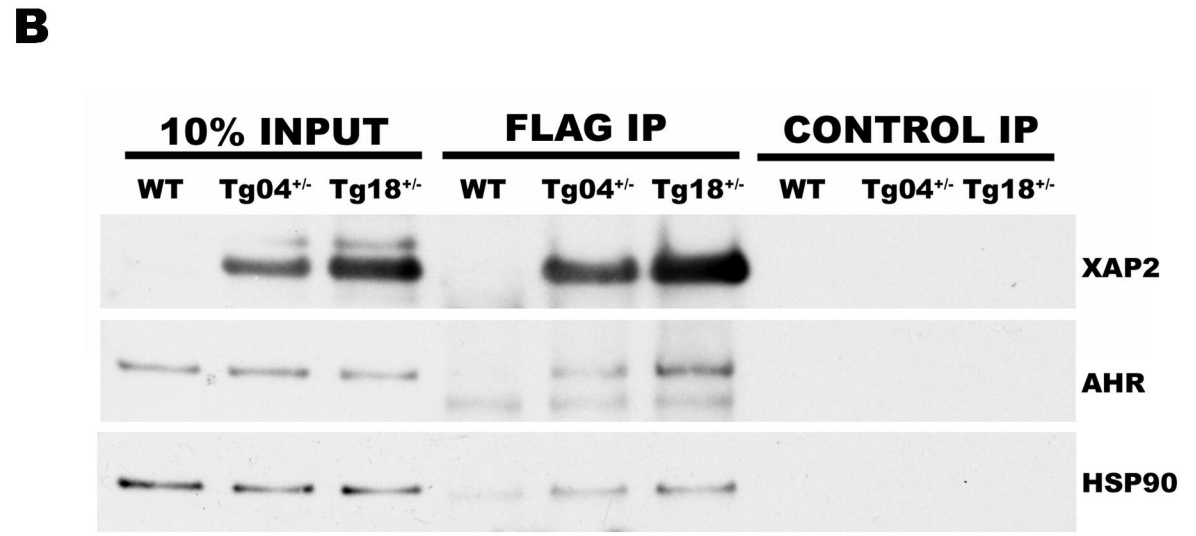

Figure 3

Molecular Pharmacology Fast Forward. Published on September 20, 2006 as DOI: 10.1124/mol.106.029215
This article has not been copyedited and formatted. The final version may differ from this version.

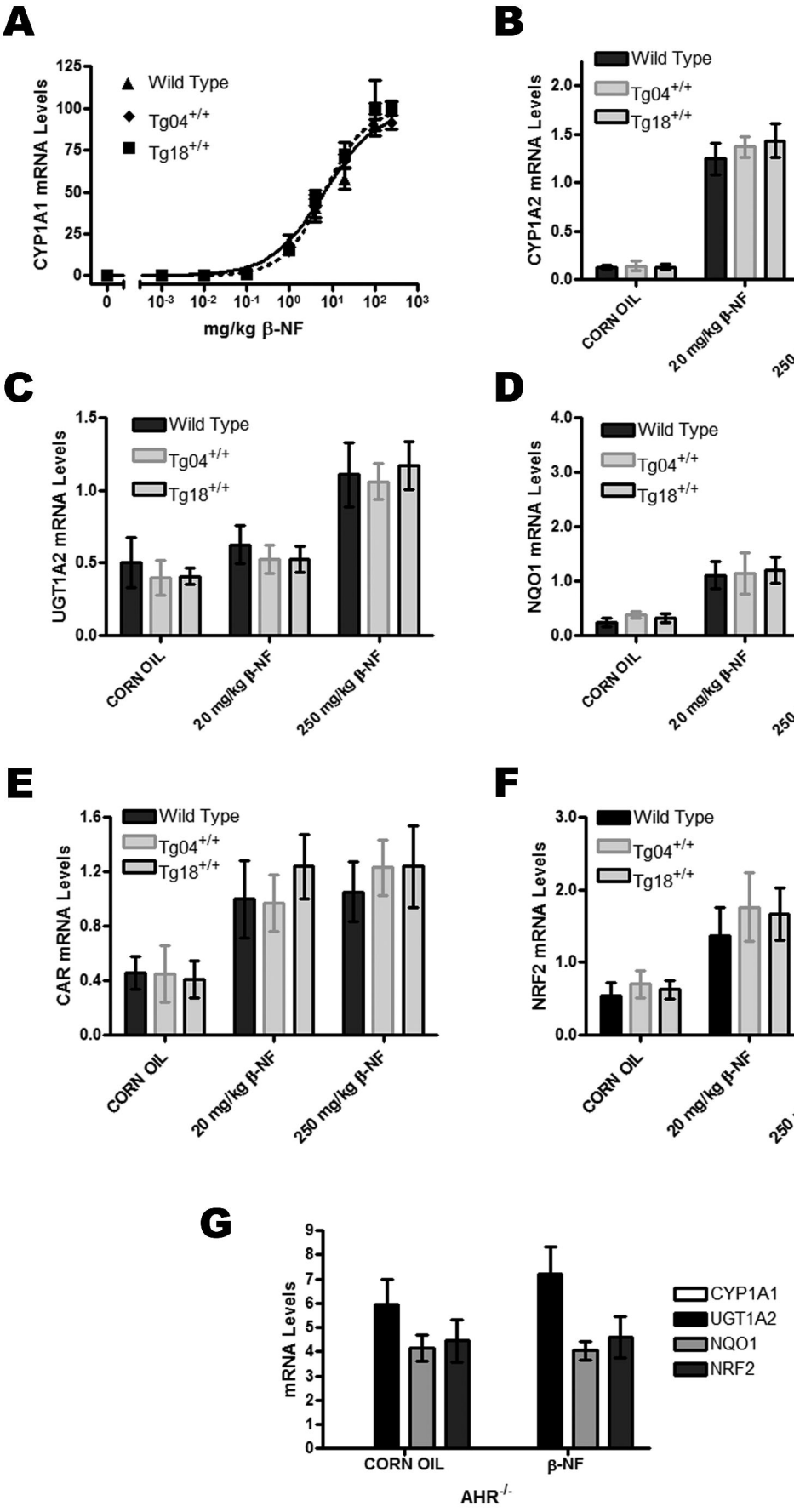

Molecular Pharmacology Fast Forward. Published on September 20, 2006 as DOI: 10.1124/mol.106.029215
This article has not been copyedited and formatted. The final version may differ from this version.

Figure 4

A

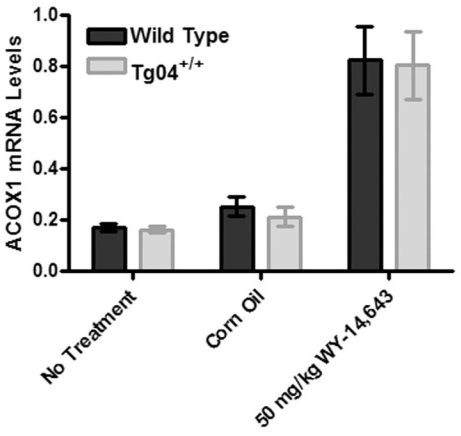

B

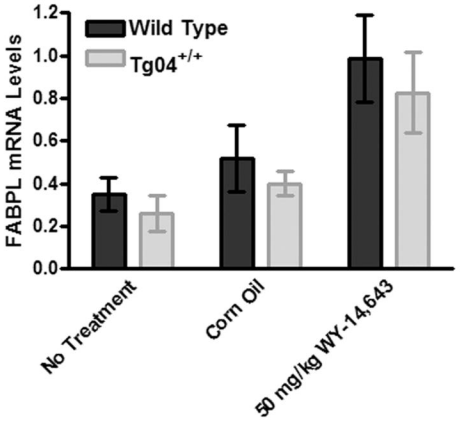

Figure 5

Molecular Pharmacology Fast Forward. Published on September 20, 2006 as DOI: 10.1124/mol.106.029215
This article has not been copyedited and formatted. The final version may differ from this version.

A

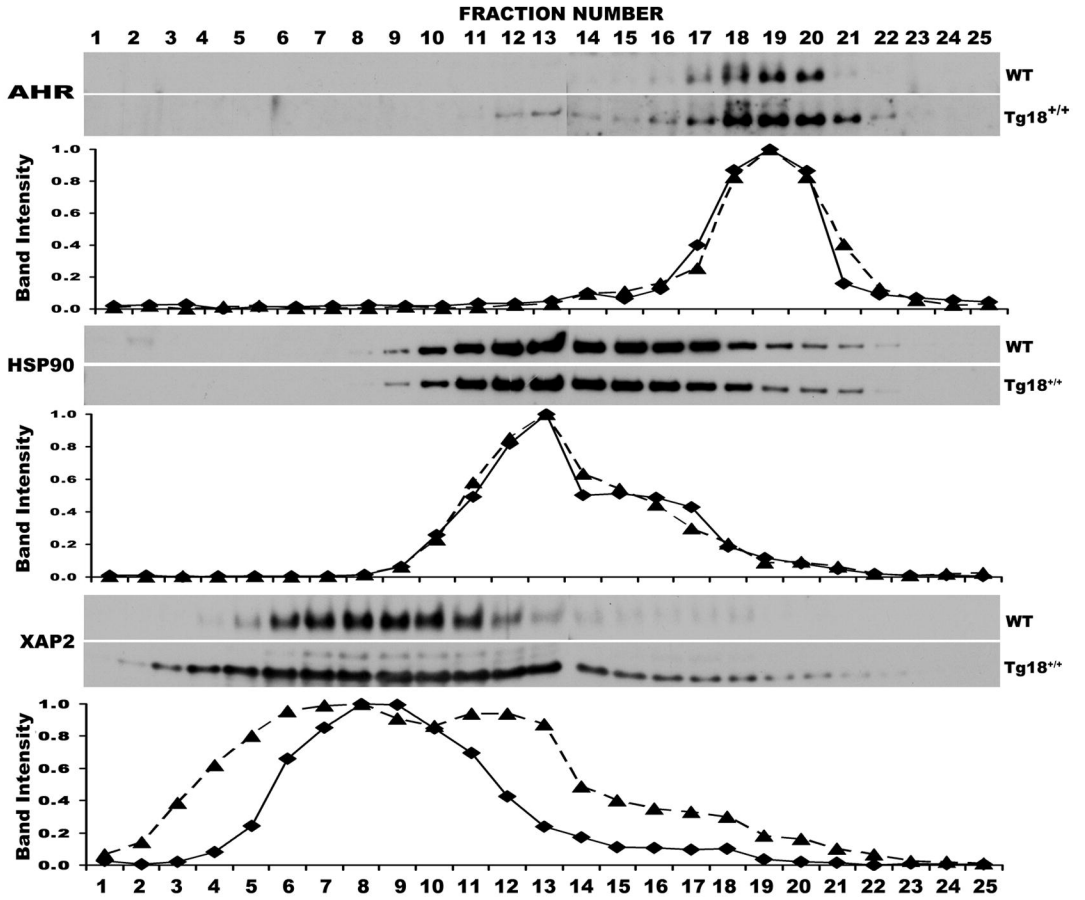

B

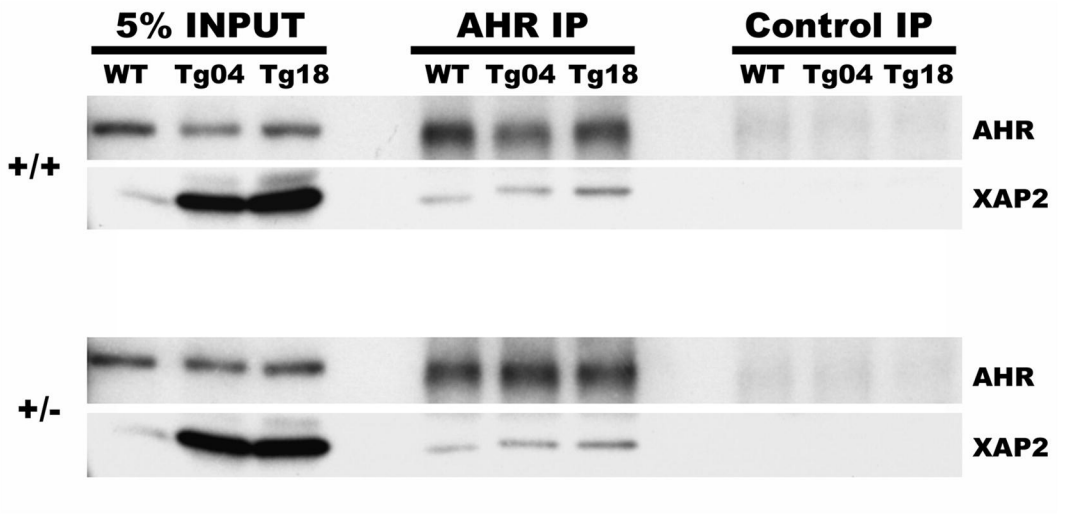

Figure 6

Molecular Pharmacology Fast Forward. Published on September 20, 2006 as DOI: 10.1124/mol.106.029215
This article has not been copyedited and formatted. The final version may differ from this version.

A

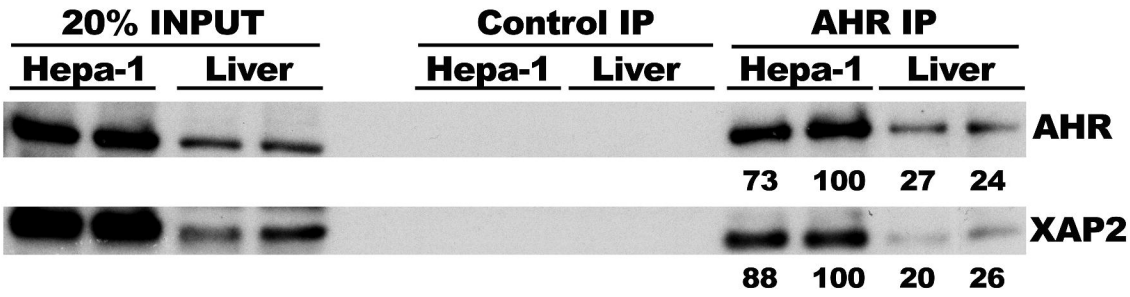

B

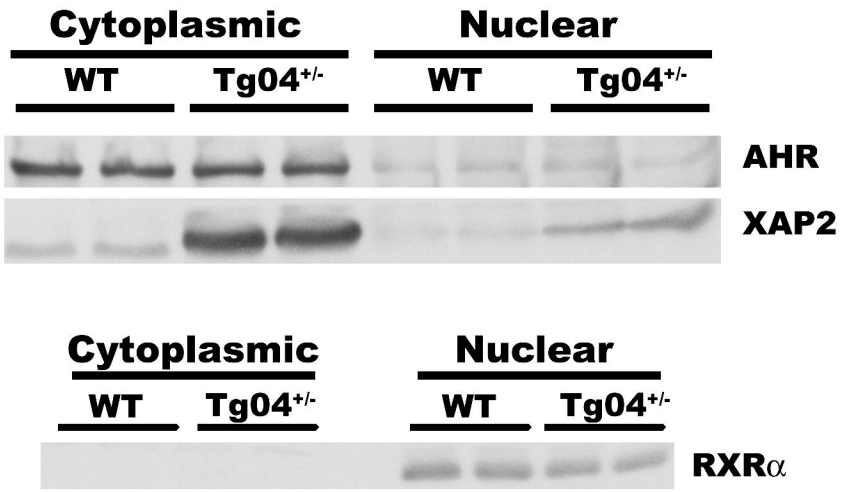

Molecular Pharmacology Fast Forward. Published on September 20, 2006 as DOI: 10.1124/mol.106.029215
This article has not been copyedited and formatted. The final version may differ from this version.

Figure 7